Modelling the impact of configurational entropy on the stability of amorphous SiO2

Owen, Megan; Rushton, Michael; Cooper, Michael William; Ghardi, Mehdi; Claisse, Antoine; Lee, Bill; Middleburgh, Simon

Scripta Materialia

DOI:
10.1016/j.scriptamat.2023.115507

Published: 01/08/2023

Peer reviewed version

Modelling the impact of configurational entropy on the stability of amorphous SiO_2

Megan W. Owen[a,*], Michael J.D. Rushton[a], Michael W. D. Cooper[c], E.M. Ghardi[a], Antoine Claisse[a,b], William E. Lee[a], Simon C. Middleburgh[a**]

[a] *Nuclear Futures Institute, School of Computer Science and Electronic Engineering, Bangor University, Bangor, Gwynedd, LL57 1UT*

[b] *Westinghouse Electric Sweden AB, 721 63 Västerås, Sweden*

[c] *Materials Science and Technology Division, Los Alamos National Laboratory, P.O. Box 1663, Los Alamos, NM 87545, USA*

**megan.owen@bangor.ac.uk*

***s.middleburgh@bangor.ac.uk*

Abstract

Configurational entropy has been computed to assess its impact on stabilizing the amorphous structure of SiO_2. Using a range of atomic scale modelling methods, the structure of crystalline and amorphous SiO_2 has been assessed and the configurational entropy associated with the structures observed at varying temperatures has allowed computation of the associated Shannon entropy. Combined with the enthalpy terms generated from density functional theory, a robust method for assessing the stability of crystalline and amorphous structures has been presented that can be used in future work assessing the role of dopants, glass forming additions and radiation damage. Future work will include the vibrational entropy term, to capture the full entropic contribution to amorphisation.

Keywords: Shannon entropy; energy of amorphisation; atomic scale modelling; SiO_2

Amorphous SiO_2 is used in the microelectronics and semiconductor industry [1] as well as being the base material for most glass systems. Amorphous SiO_2 is formed of corner sharing tetrahedral SiO_4 units, consistent with crystalline SiO_2 but lacking long-range order. Modifications to the periodic structure also exist in simulated amorphous SiO_2, with non-bridging oxygens and under/over coordinated Si ions present in the systems due to unphysical quench rates observed in simulation studies [2]. Amorphisation of crystalline oxides such as

SiO_2 can occur due to irradiation, as well as quenching from the liquid state [3]. Gaikwad *et al.* [4] found experimentally that increasing fluence of swift heavy ions caused polycrystalline SiO_2 to become amorphous, alongside decreasing the electrical conductivity of the film.

The impact of structure and temperature has been analysed here in terms of the system's configurational entropy. Smith *et al.* [5] found the difference in entropy between metallic crystalline and glassy systems was entirely configurational. However, Johari [6] found vibrational entropy is a contributing factor to overall entropy in a glassy system. Richet [7] analysed the vibrational and configurational entropies of SiO_2 systems, showing that glassy SiO_2 systems had a lower vibrational entropy than the crystalline counterpart. For this work, configurational entropy is the main entropic factor, with future adaptations to the method including vibrational entropy terms.

Enthalpy terms were calculated to compute the Gibbs free energy for each system. The ease of amorphization has been analysed for crystalline polymorphs of SiO_2 considered. This model aims to predict the behaviour of amorphous phase formation, to be coupled with experimental works in future.

The development of a novel theoretical model to calculate the tendency towards the formation of amorphous SiO_2 is presented. The method described is a four-step approach to calculating the Gibbs free energy of amorphisation.

1) Calculating the configurational entropy of the systems at successive temperature increments using molecular dynamics and Voronoi tessellation. The number of faces of Voronoi polyhedral provides the configurational entropy term. Tessellations are based on the building blocks of the SiO_2 system, analysing only Si – O and O – Si pairs, novel to this work, especially for amorphous oxide systems.

2) Calculating the enthalpies using density functional theory.

3) Calculating the Gibbs free energy of the systems at temperature using Equation 3, combining both MD and DFT results.

4) Calculating the Gibbs free energy of amorphization by calculating the difference in Gibbs free energies between crystalline and amorphous SiO_2 systems.

Atomsk [8] was used to generate supercells of the α-quartz and β-cristobalite polymorphs of SiO_2 (5184 atoms). The SiO_2 systems in this work were described using the Munetoh potential, a short-range Tersoff potential, and has been used successfully to describe crystalline and amorphous SiO_2 systems [9].

A simulated melt-quench was used to generate the amorphous systems, conducted using classical molecular dynamics (MD). The Large-scale Atomic/Molecular Massively Parallel (LAMMPS) package was used for all MD simulations described herein [10]. The β-cristobalite polymorph was used as a starting structure for the SiO_2 melt-quench. The systems were heated using in the isothermal-isobaric (NPT) ensemble, from 300 K to 5000 K over 100 ps, and then held at 5000 K for 100 ps to ensure the systems had fully melted. The systems were then quenched at a rate of 0.4 K/ps in an NPT ensemble, using incremental 100 K ramps to lower temperatures over 20 ps, and further equilibration at temperature for 20 ps. Upon reaching 300 K, the systems were held for a further 100 ps using the NPT ensemble for equilibration purposes. Time-averaged radial distribution functions were calculated for the equilibrated structures.

The structures of α-quartz and β-cristobalite were equilibrated at 300 K over 2000 ps. MD was used to heat all systems from 300 K to 1500 K, to analyse a temperature range before melting (1723 °C (1996.15 K) [11]). Ten different structures for each system were heated in increments of 100 K using the NPT ensemble, over 20 ps. Smaller increments of 10 K were used by Cowen and El-Genk [12], in which the α-quartz to β-cristobalite transition was captured successfully. This has not been used here due to the large volume of data required for this work. Capturing the transition does not impact the conclusions made in terms of analysing the configurational entropy of the crystalline polymorphs.

The systems were then held at the temperature for a further 20 ps, before being ramped further. The equilibrated structure at 100 K increments was used to provide a snapshot of the system at different temperatures. At each temperature, the voro++ software [13], was used to calculate the Voronoi tessellations of the systems. Voronoi polyhedral were generated for each ion in the system, partitioning the supercell into Voronoi domains. For each atom in the cell, the number of faces of the Voronoi domain was calculated. The number of faces of the Voronoi polyhedral provides the number of nearest neighbours. In this work, Si – O and O –

Si pairs were analysed, by filtering Si – Si and O – O pairs from the data. This method was used to capture the building blocks of the SiO_2 systems. The number of faces of the Voronoi polyhedral has been used as a measure of configurational entropy at each temperature, through the computation of the Shannon entropy.

The Shannon entropy is a measure of information and uncertainty, commonly used in information theory [14], given by Equation 1, where x_i denotes a specific number of Voronoi faces of a polyhedral, and $p_i(x_i)$ is the probability of occurrence of a specific number of Voronoi faces of a polyhedron. A conversion to Gibbs' entropy is made by including Boltzmann's constant, k_B, as shown in Equation 2. The Gibbs entropy is used in statistical thermodynamics, providing an accurate configurational entropy term for these systems.

$$S_{Shannon} = -\sum_{i=1}^{n} p_i(x_i)\log\big(p_i(x_i)\big) \tag{1}$$

$$S_{Gibbs} = -k_B\sum_{i=1}^{n} p_i(x_i)\log p_i(x_i) \tag{2}$$

Vibrational entropy was also considered when analysing the configurational entropy. In the quasi-harmonic approximation, vibrational entropy can be expressed by the relation:

$$S_{vib} = 3k_B\int_0^{\infty} g(E)([1+n(T)]\ln[1+n(T)] - n(T)\ln\ n(T))dE \tag{3}$$

Where $n(T) = \left(\exp\left(\frac{E}{k_BT}\right) - 1\right)^{-1}$ is the Planck distribution for phonon occupancy and $g(E)$ is the phonon density of states (DOS). To assess numerically the vibrational entropy in this work, the vibrational density of states was calculated at temperatures from 300K to 1500K using lattice dynamics formalism. In this formalism, each normal mode i can be characterized by a frequency ω^i and a polarization vector $\vec{e}^{\,i}$ which are obtained from the diagonalisation of the dynamical matrix expressed as:

$$D^{\alpha\beta}e^{i,\alpha} = (\omega^i)^2 e^{i,\beta} \tag{4}$$

Once the eigenvalues and eigenvectors are obtained, the VDOS can be obtained by building histograms of the frequencies ω^i.

Density functional theory (DFT) has been used to calculate the enthalpy terms, using the Vienna Ab-initio Simulation Package (VASP) [15]. Ten different structures were used for each system. Smaller cells of 72 atoms for the crystalline systems were generated using the Atomsk software. For amorphous systems, Reverse Monte Carlo (RMC) calculations were conducted using the RMC_POT software [16]. RMC structurally minimises the supercells used in MD (5184 atoms) to smaller cells (72 atoms) conforming with input radial distribution function (RDF) data from the MD generated supercells [17]–[19].

The smaller cells were used as input data for the DFT calculations. All 10 systems were structurally relaxed and the DFT relaxed radial distribution functions were compared with that of the MD and Atomsk/RMC data, to ensure consistency in structures. The GGA-PBE was used, alongside the PAW potential library [20], [21]. Collinear calculations were conducted, and a cut-off energy of 500 eV was used. Ionic relaxation calculations were conducted using damped molecular dynamics, alongside allowing ionic positions, cell shapes, and cell volumes to fully relax. The self-consistent stopping criterion was set to 1×10^{-4} eV, and the ionic relaxation stopping criterion was set to 1×10^{-3} eV. A Monkhorst-Pack scheme was used to set a $3 \times 3 \times 3$ k-point grid.

The Gibbs free energy for each system was calculated using Equation 5, where G is the Gibbs free energy in eV, H is the enthalpy in eV, T is the temperature in K, and S is the configurational entropy in eV/K.

$$G = H - TS \tag{5}$$

A difference in Gibbs free energy was directly calculated between the amorphous and crystalline systems to calculate the free energy of amorphization between the two counterparts.

Crystalline and amorphous SiO_2 systems were generated successfully (Figure 1). Radial distribution functions generated for crystalline SiO_2 are periodic. The system is affected at longer separation distances due to the potential used being a short-range potential. The amorphous SiO_2 radial distribution function is characteristic of that of a disordered system, with two prominent peaks at 1.63 Å and 2.68 Å before tailing off at a value of g(r) equal to 1.

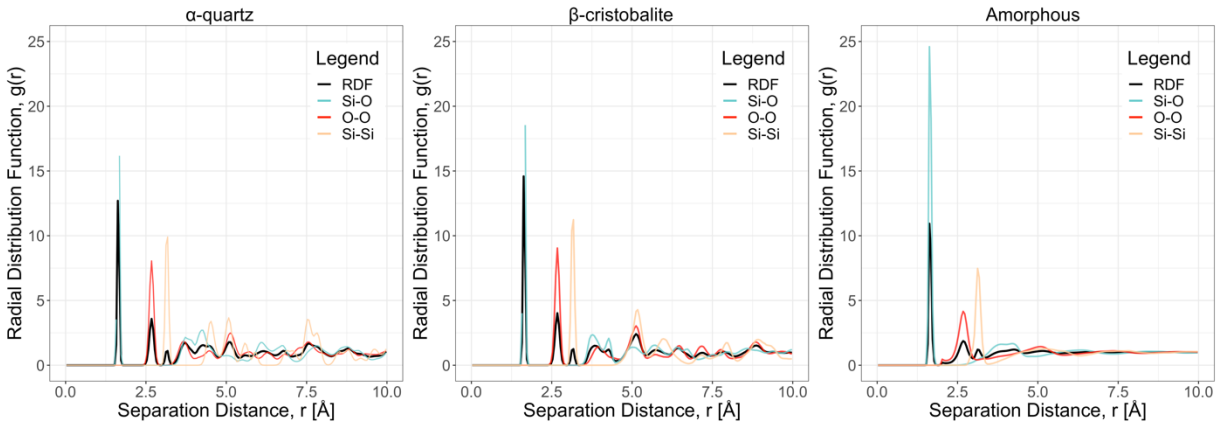

Figure 1: Radial distribution function and partial radial distribution functions for a) α-quartz, b) β-cristobalite, and c) amorphous SiO_2 systems at 300 K.

Histograms were formed of the number of faces of the Voronoi polyhedral observed in crystalline and amorphous SiO_2 systems, at 300 K and 1500 K (Figure 2). The histograms shown are averaged over 10 simulation runs for each system.

For the crystalline systems, a prominent peak was observed for number of faces of oxygen and silicon ion polyhedral at 300 K. For both crystalline polymorphs, the modal number of faces for Voronoi polyhedral of oxygen and silicon ions was 3 and 7 respectively. The numbers are decreased here than that expected for the SiO_2 system (O – Si coordination = 4, and Si – O coordination = 8), which can be related to the equilibration of the system at temperature. As the temperature is increased to 1500 K, the distribution broadens for both oxygen and silicon ion Voronoi polyhedral. A wider range of coordination environments are observed, relating well with that expected at increased temperature.

For the α-quartz polymorph, the modal number of faces for oxygen and silicon ion polyhedral remain unchanged with temperature. For the β-cristobalite polymorph, the modal number of

faces for the silicon ion Voronoi polyhedral decreases to 6, with oxygen unchanged. The decrease in the modal number of silicon faces for the β-cristobalite polymorph can be related to the temperature effects, alongside the polymorph structure. With increased temperature, ions within the system gain energy and are therefore able to migrate within the cell. SiO_4 tetrahedra in the quartz polymorphs are more densely packed in comparison to the cristobalite polymorph [22], accounting for the decreased coordination number observed here. Despite the modal numbers remaining mostly unchanged, a broadening of the histogram is observed, indicative of higher disorder than that observed at 300 K.

For the amorphous systems, a broad range of faces is observed for both oxygen and silicon ion polyhedral at both temperatures. No changes to the modal number of faces are observed at higher temperatures, indicating that the disordered system is observed at both temperatures.

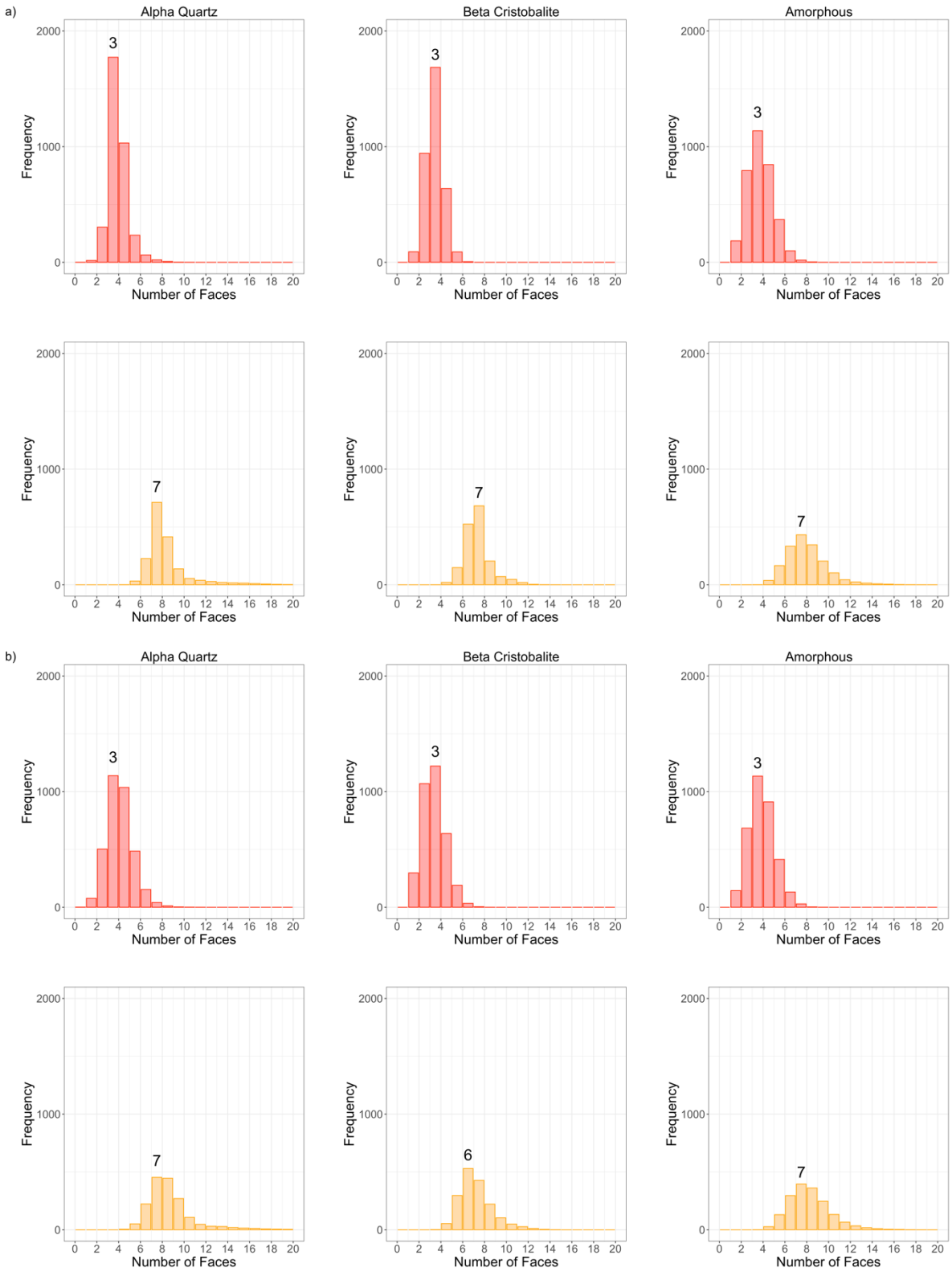

Figure 2: Histograms of number of faces for oxygen (red) and silicon (orange) Voronoi polyhedral at a) 300 K, and b) 1500 K, in α-quartz (left), β-cristobalite (centre), and amorphous (right) SiO_2.

Configurational entropy and Gibbs free energy was calculated successfully for the SiO_2 systems (Figure 3). Crystalline polymorphs have a lower configurational entropy than the amorphous system, due to crystallinity effects. Both crystalline systems have a lower Gibbs free energy, with these systems more favourable to form in comparison to the amorphous counterpart.

Comparisons between MD and DFT simulated systems have been made (Table 1). Energies and enthalpies of each structure has been computed at 0 K, as entropy and enthalpy are lowest at this temperature. The results are averaged over 10 simulation runs. Standard error has been included, and terms without standard error included are due to the error being negligible. A deviation between MD and DFT values is observed, related to the different potential used for both sets of simulations.

Table 1: Energy and enthalpy of the MD and DFT simulated silica systems per SiO_2 unit.

Energy [eV]			
	α-quartz	β-cristobalite	Amorphous
MD	-20.09	-19.61	-19.74 ± 0.05
DFT	-23.71	-23.71	-22.77 ± 0.03
Enthalpy [eV]			
MD	-19.38	-17.41	-19.80 ± 0.1
DFT	-23.71	-23.71	-22.77 ± 0.03

For the α-quartz system, no change in lattice parameters or Gibbs free energy is observed, to indicate a change in polymorph. For the β-cristobalite system, initially, the lattice parameters are not equal (a≠b≠c) but become equal (a=b=c) at 800 K, and remain equal until melting. This is indicative of the cubic β-cristobalite structure. No change in Gibbs free energy is captured in Figure 3b relating to the change in lattice parameter. The polymorphic transformation is captured when analysing the vibrational entropy, discussed later in the manuscript.

As temperature is increased in crystalline SiO_2 systems, the configurational entropy increases, due to atoms oscillating about their positions within the systems. The configurational entropy of the α-quartz system approaches that of the amorphous system, which may be due to the system approaching a melt phase. This is reasonable, as α-quartz polymorph is the low temperature polymorph for SiO_2. For the β-cristobalite polymorph, the configurational entropy is lower than the α-quartz polymorph, due to β-cristobalite being the high temperature polymorph [11].

In our model, the Gibbs free energy of β-cristobalite remains similar to that of α-quartz up to high temperatures. A cross over in Gibbs free energy is observed at approximately 1490 K. This result indicates that the inclusion of other entropy terms to reliably predict the observed phase transformation is required and is found later in the manuscript.

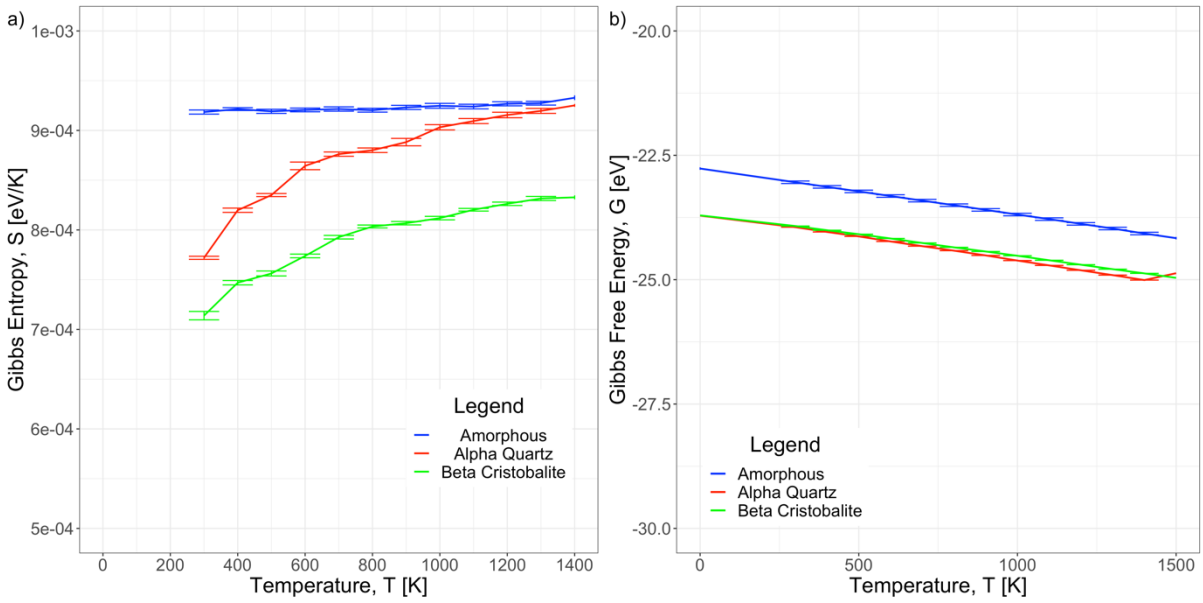

Figure 3: a) Configurational entropy, and b) Gibbs free energy of crystalline and amorphous SiO_2.

Vibrational entropy of the SiO_2 systems was computed successfully. Magnitudes of vibrational entropy were lower than that observed for configurational entropy and can therefore be neglected when computing the Gibbs free energy. However, vibrational entropy is important in capturing polymorphic changes (Figure 4). For crystalline polymorphs, a steep increase in vibrational entropy is observed at approximately 1100 – 1200 K (Figure 4), indicative of a polymorphic transition.

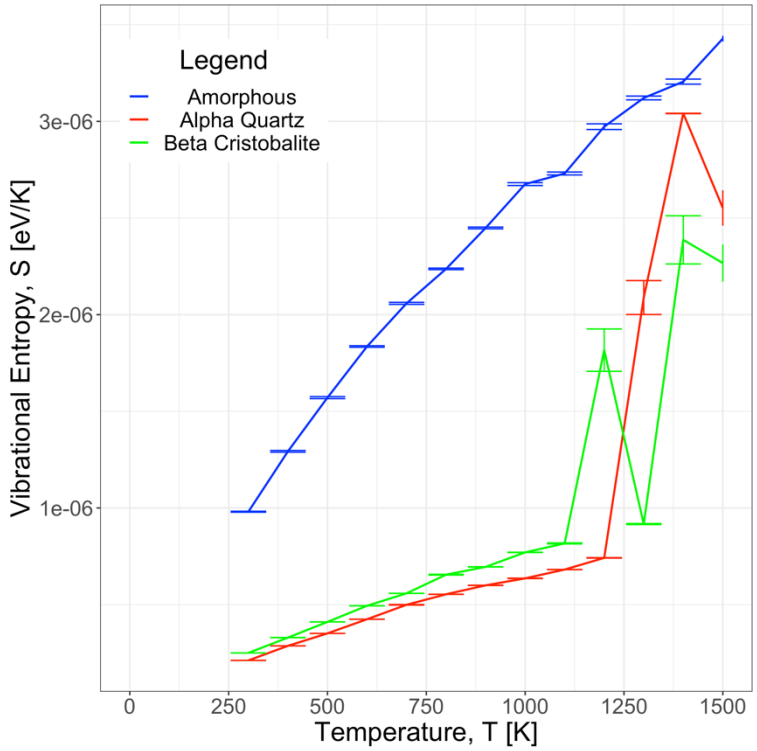

Figure 4: Vibrational entropy of crystalline and amorphous SiO_2 between 300 K and 1500 K.

RMC and DFT calculations were conducted successfully on the SiO_2 systems. Energies of amorphization were calculated successfully (Figure 5) using the configurational entropy terms calculated using MD, and enthalpy terms calculated using DFT.

The Gibbs free energy of amorphisation is unfavourable for both crystalline polymorphs simulated here, within the temperature range simulated. No external factors have been considered for this work, such as irradiation or defects. The amorphisation of β-cristobalite is more favourable than α-quartz, especially at temperatures above 600 K. Richet [23] found that above 1200 K, cristobalite polymorphs were more favourable to form glassy systems, relating well with that shown in Figure 5. At lower temperatures, the quartz system was most favourable to form a liquid or glassy SiO_2 system, over the cristobalite [23]. This cross over in favourability is not observed in Figure 5, however, a cross over in vibrational entropy of the crystalline polymorphs above 1200 K is observed in Figure 4. Further developments to the model would include vibrational entropy terms, to capture the full progression and impact of phase transformations.

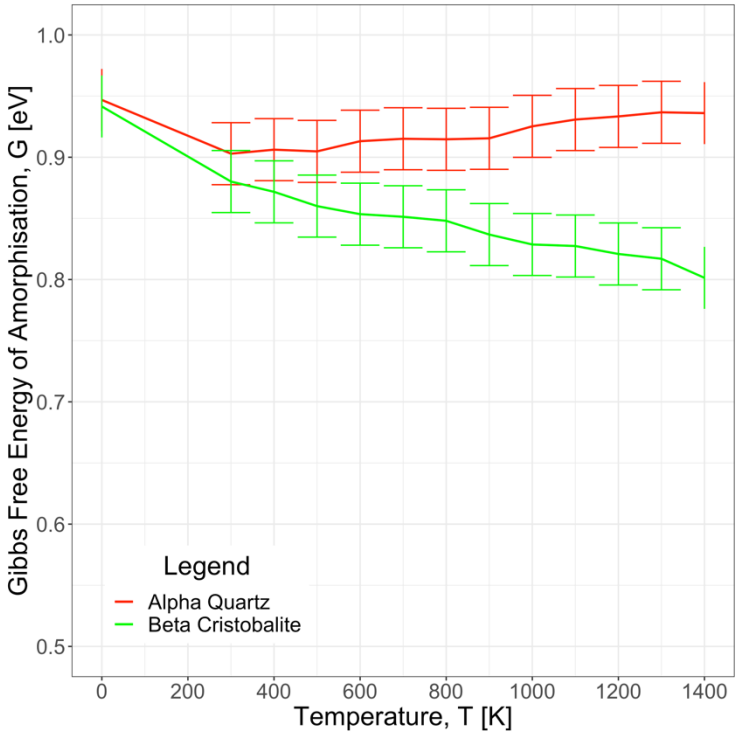

Figure 5: Gibbs free energy of amorphisation for α-quartz and β-cristobalite polymorphs of SiO_2.

A range of modelling methods have been used successfully to calculate the Gibbs free energy and Gibbs free energy of amorphization for SiO_2, using the novel method proposed here. Without the presence of external factors to induce amorphization, crystalline polymorphs of SiO_2 will remain favourable to form up until melting temperatures.

Future work will include incorporating the vibrational entropy term into the model. Further analysis of vibrational entropy is required to develop a better understanding of the Gibbs free energy of the SiO_2 system. Polymorph transformations would be better predicted, such as the α-quartz to β-cristobalite transition. Future works will also analyse the changing configurational entropy due to melting in both amorphous and crystalline systems.

Acknowledgements

This work has been carried out as part of a KESS 2 funded PhD project, with industrial sponsors being Westinghouse Springfields Ltd. Knowledge Economy Skills Scholarships (KESS 2) is a pan-Wales higher level skills initiative led by Bangor University on behalf of the HE sector in Wales. It is part funded by the Welsh Government's European Social Fund (ESF) convergence programme for West Wales and the Valleys. SCM, WEL and MJDR are funded through the Sêr

Cymru II programme by Welsh European Funding Office (WEFO) under the European Development Fund (ERDF). Computing resources were made available by HPC Wales and Supercomputing Wales, alongside EPSRC Tier 2 National HPC Services hosted by the University of Cambridge.

The data that support the findings of this study are available on request from the corresponding author.

References

[1] V. Astašauskas, A. Bellissimo, P. Kuksa, C. Tomastik, H. Kalbe, and W. S. M. Werner, "Optical and electronic properties of amorphous silicon dioxide by single and double electron spectroscopy," *J Electron Spectros Relat Phenomena*, vol. 241, May 2020, doi: 10.1016/j.elspec.2019.02.008.

[2] A. v. Sulimov, D. C. Kutov, F. v. Grigoriev, A. v. Tikhonravov, and V. B. Sulimov, "Generation of Amorphous Silicon Dioxide Structures via Melting-Quenching Density Functional Modeling," *Lobachevskii Journal of Mathematics*, vol. 41, no. 8, pp. 1581–1590, Aug. 2020, doi: 10.1134/S1995080220080193.

[3] D. M. Mattox, "Atomistic Film Growth and Some Growth-Related Film Properties," in *Handbook of Physical Vapor Deposition (PVD) Processing*, Second Edition., William Andrew Applied Science Publishers, 2010, pp. 333–398.

[4] A. Gaikwad, Y. Mhaisagar, S. Gupta, B. Joshi, K. Asokan, and A. Mahajan, "Amorphization of SiO_2 Thin Films by Using 200 MeV Ag 15+ Ions," *Silicon*, vol. 11, no. 2, pp. 1017–1021, Apr. 2019, doi: 10.1007/s12633-018-9882-4.

[5] H. L. Smith *et al.*, "Separating the configurational and vibrational entropy contributions in metallic glasses," *Nat Phys*, vol. 13, no. 9, pp. 900–905, Sep. 2017, doi: 10.1038/nphys4142.

[6] G. P. Johari, "Contributions to the entropy of a glass and liquid, and the dielectric relaxation time," *Journal of Chemical Physics*, vol. 112, no. 17, pp. 7518–7523, May 2000, doi: 10.1063/1.481349.

[7] P. Richet, "Viscosity and configurational entropy of silicate melts," *Geochim Cosmochim Acta*, vol. 48, no. 3, pp. 471–483, 1984, doi: 10.1016/0016-7037(84)90275-8.

[8] P. Hirel, "Atomsk: A tool for manipulating and converting atomic data files," *Comput Phys Commun*, vol. 197, pp. 212–219, 2015, doi: 10.1016/j.cpc.2015.07.012.

[9] S. Munetoh, T. Motooka, K. Moriguchi, and A. Shintani, “Interatomic potential for Si-O systems using Tersoff parameterization,” *Comput Mater Sci*, vol. 39, no. 2, pp. 334–339, Apr. 2007, doi: 10.1016/j.commatsci.2006.06.010.

[10] A. P. Thompson *et al.*, “LAMMPS - a flexible simulation tool for particle-based materials modeling at the atomic, meso, and continuum scales,” *Comput Phys Commun*, vol. 271, Feb. 2022, doi: 10.1016/j.cpc.2021.108171.

[11] J. F. Shackelford, *Introduction to Materials Science for Engineers*, 6th ed. Prentice-Hall, 2005.

[12] B. J. Cowen and M. S. El-Genk, “On force fields for molecular dynamics simulations of crystalline silica,” *Comput Mater Sci*, vol. 107, pp. 88–101, 2015, doi: 10.1016/j.commatsci.2015.05.018.

[13] C. H. Rycroft, “VORO++: A three-dimensional Voronoi cell library in C++,” *Chaos*, vol. 19, no. 4, pp. 1–16, 2009, doi: 10.1063/1.3215722.

[14] L. Masisi, V. Nelwamondo, and T. Marwala, “The use of entropy to measure structural diversity,” *ICCC 2008 - IEEE 6th International Conference on Computational Cybernetics, Proceedings*, pp. 41–45, 2008, doi: 10.1109/ICCCYB.2008.4721376.

[15] G. Kresse and J. Hafner, “Ab initio molecular dynamics for liquid metals,” *Phys Rev B*, vol. 47, no. 1, pp. 558–561, 1993.

[16] O. Gereben and L. Pusztai, “RMC-POT: A computer code for reverse monte carlo modeling the structure of disordered systems containing molecules of arbitrary complexity,” *J Comput Chem*, vol. 33, no. 29, pp. 2285–2291, Nov. 2012, doi: 10.1002/jcc.23058.

[17] D. M. Ramo, A. Chroneos, M. J. D. Rushton, and P. D. Bristowe, “Effect of trivalent dopants on local coordination and electronic structure in crystalline and amorphous ZnO,” *Thin Solid Films*, pp. 1–5, 2013, doi: 10.1016/j.tsf.2013.05.140.

[18] M. J. D. Rushton, I. Ipatova, L. J. Evitts, W. E. Lee, and S. C. Middleburgh, “Stoichiometry deviation in amorphous zirconium dioxide,” *RSC Adv*, vol. 9, no. 29, pp. 16320–16327, 2019, doi: 10.1039/c9ra01865d.

[19] S. C. Middleburgh, W. E. Lee, and M. J. D. Rushton, “Structure and properties of amorphous uranium dioxide,” *Acta Mater*, vol. 202, pp. 366–375, Jan. 2021, doi: 10.1016/j.actamat.2020.10.069.

[20] J. P. Perdew and W. Yue, “Accurate and simple density functional for the electronic exchange energy: Generalized gradient approximation,” *Phys Rev B*, vol. 33, no. 12, pp. 8800–8802, 1986.

[21] G. Kresse and D. Joubert, “From ultrasoft pseudopotentials to the projector augmented-wave method,” *Phys Rev B*, vol. 59, no. 3, pp. 1758–1775, 1999.

[22] “The Product Solid Phases,” in *Developments in Geochemistry*, vol. 11, 2007.

[23] P. Richet, “Superheating, melting and vitrification through decompression of high-pressure minerals,” Wiley, 1983.